MODELLING FOULING INDUCTION PERIODS

Mengyan Yang*, Andrew Young, Amir Niyetkaliyev, and Barry Crittenden

Department of Chemical Engineering

University of Bath, Bath, UK, BA2 7AY

Telephone: (44) 01225 386501
*corresponding author: my223@bath.ac.uk

ABSTRACT

A fouling process is often preceded by an induction period in which no significant fouling is observed. In this paper, a simple lumped parameter model based on fractional surface coverage θ has been developed to correlate experimental data in the induction period. The model assumes that active foulant species stick to the surface and gradually cover it, the rate of change of surface coverage $d\theta/dt$ being proportional to the fractional free surface ($1-\theta$). It is further assumed that the foulant already on the surface acts as a seed, attracting more foulant in a micro-growth manner such that the growth rate is first order in θ with a rate constant k_1. Adopting the concept of removal mechanism similar to that used in adsorption science, the removal rate of the coverage is set to be proportional to the coverage with a rate constant of k_2. The three assumptions are combined to obtain the relationship $d\theta/dt = k_1\theta(1- \theta) – k_2\theta$. The fouling layer grows on the covered surface and the fouling rate can be expressed as $\theta R_f'$ where R_f' can be any established fouling rate expression. Experimental data, including data obtained during induction periods have been successfully correlated for systems including crude oil fouling, water scaling and whey protein fouling. The physical meanings of the model parameters are discussed. The model supports experimental observations in which shorter induction periods are found with higher surface temperatures. The effects of the surface material and the flow velocity are also analysed.

Keywords**:** Fouling**,** induction period, thermal resistance, crude oil, water scaling, whey protein.

NOMENCLATURE

A	Constant in Yeap et al. model (Eq. (16))
A_i	pre-exponential factor, 1/s
B	Constant in Yeap et al. model (Eq. 16)
C_f	Friction factor
c	constant of integration

E_i	activation energy for induction period, kJ/mol
E	activation energy in Yeap et al. model (Eq. (16)), kJ/mol
G	free energy, kJ/mol
k_1 *and* k_2	lumped rate constants, 1/s
R_a	absolute surface roughness, μm
R	universal gas constant, 8.314J/mol K
Re	Reynolds number
R_f and R_d	fouling resistance, m^2K/kW
R_f'	fouling rate, m^2K/kJ
T	absolute surface temperature, K
t	time, hour, min, or s
$t_{0.5}$	time when $d\theta/dt$ is a maximum, the induction time or induction period length
u	velocity, m/s
γ	model constant for k_2, $m^{-0.8}s^{-0.2}$ or dimensionless
θ	fractional surface coverage
θ_{max}	maximum fractional surface coverage
μ	fluid viscosity, Pa s
ρ	fluid density, kg/m^3

1. INTRODUCTION

Fouling is commonly preceded by an induction (or initiation period) in which no significant change of thermal resistance is observed with increasing time, with exception of fouling under boiling conditions. The induction period could be from a few minutes in a laboratory experiment to a month or so in refinery equipment. A number of researchers have addressed the induction period phenomenon under non-boiling conditions for a wide range of fouling mechanisms. For example, the induction period for protein fouling has been studied in some depth. Belmar-Beiny et al. [1] observed a much shorter induction period in a plate heat exchanger than in a tubular heat exchanger. They considered that this was due to the higher

turbulence in the former. Belmar-Beiny and Fryer [2] analysed the first layer of deposit which was thought to be formed during the induction period, and found that it was made of proteinaceous materials rather than minerals. Geddert et al. [3] investigated the effects of surface coatings and attempted to correlate the induction with the surface roughness and surface tension but did not reach any quantitative conclusion. Augustin et al. [4] investigated the effect of surface treatments on protein fouling and reported the effect of surface temperature on the induction period. In spite of many observations and investigations of induction phenomena, this period in a fouling process has not been studied in a substantially quantitative manner, and this is certainly the case for crude oil fouling. The main reason for this can be attributed not only to the complexity of the fouling behaviour in the induction period but also to the fact that no additional experimental information can be gained when the induction period occurs, since it appears as a steady state phenomenon in which no useful experimental data can be collected.

Whilst most fouling models focus on the fouling rate when the heat transfer resistance is increasing (e.g. Wilson et al. [5]), few models address the preceding induction period. Vatistas [6] reported a stochastic model for the induction step in particulate fouling. This model can predict the effect of friction velocity on induction time, but was found to be difficult to use in correlating experimental data. Malayeri and Müller-Steinhagen [7] developed a phenomenological model for the prediction of fouling resistance of calcium sulphate solutions during boiling heat transfer, including an empirical estimation of the induction time. However, this model, as they stated, is only limited to the fouling period and it was recommended that one should endeavour to correlate data within the initial period. Neural network techniques have been successfully used to correlate the data during the entire fouling process [7, 8] but the drawback of this approach is that it is, in essence, a black box technique which does not offer any physical understanding of the process. Fahiminia et al. [9] derived a relationship between delay time (i.e. induction period) and supersaturation ratio at any given fluid velocity and surface temperature based on classical nucleation theory. They also showed that for any given fluid velocity and surface temperature, there is an Arrhenius

relationship between the reciprocal of the delay time and the surface temperature. However applications of their approach may be limited to crystallization fouling. Moreover, it could be difficult to measure or determine the delay time as there is rarely a sharp boundary between the delay time and the following stage. All of these studies indicate that there is still a significant gap in physical models of the initial stages of fouling processes.

The importance of the induction period should not be underestimated. If a good knowledge existed of why induction periods occurred, then it might be possible to exploit this knowledge and extend the induction period indefinitely. A first step in understanding is to create a simple model which can account for the influence of process parameters on the induction period. In this paper, a relatively simple model is developed to correlate the data in the induction period, the related factors being considered in a lumped form. The effects of surface temperature, flow velocity and the surface on the induction period under non-boiling conditions are considered but any changes in surface roughness which might arise and hence increase the heat transfer coefficient during the induction or initiation period will be ignored.

2 MODEL DEVELOPMENT

2.1 Model assumptions and description

Fouling on a heat exchanger surface may be described in the following manner. Firstly, in the induction, initiation or pre-conditioning period, the active fouling species adhere to the heat transfer surface and gradually cover it from a fractional coverage of $\theta = 0$ to total coverage at $\theta = 1$. Here, the surface to which the fractional coverage θ refers is defined as an idealised area where the surface temperature is considered to be uniform (remove " and is measured by a specified thermocouple"). This pre-conditioning layer is very thin, though not necessarily a single molecular layer and so the increase in fouling resistance R_f is negligible. Changes in surface roughness are ignored. Secondly, in the fouling period the fouling layer may start to grow immediately on the covered/pre-conditioned surface when it may be assumed that the growth rate is proportional to θ. However, the overall fouling growth is very slow until the surface is considerably covered/pre-conditioned. The overall rate of fouling resistance growth can therefore be expressed as:

$$\frac{dR_f}{dt} = \theta R_f' \tag{1}$$

Here, R_f' can be any form of established fouling rate expression, such as those proposed by Crittenden et al. [10], Epstein [11], Ebert and Panchal [12], etc. These models describe the fouling rate in a near linear form. Table 1 lists the functions of R_f' used for the fouling rates in related figures in this paper. In the early stage of surface pre-conditioning, active species can be captured and adhered to the surface. The following relationship may then apply:

$$\frac{d\theta}{dt} \propto (1-\theta) \tag{2}$$

Meanwhile, the particles that stick to the surface act as seeds, attracting more foulant around them, such that fouling proceeds in a micro-growth manner. The growth rate is assumed to be first order in fractional surface coverage θ:

$$\frac{d\theta}{dt} \propto \theta \tag{3}$$

Combining the two aspects gives the coverage growth rate as follows:

Growth rate = $k_1\theta(1-\theta)$ (4)

Adopting the concept of removal or release from the surface as in adsorption science, the removal rate of the surface coverage is assumed to be proportional to the surface coverage. That is:

Removal rate = $k_2\theta$ (5)

Combining Eqs. (4) and (5) yields the net growth rate:

$$\frac{d\theta}{dt} = k_1\theta(1-\theta) - k_2\theta \tag{6}$$

Rearranging Eq. (6) gives:

$$\frac{d\theta}{\theta[(1-\frac{k_2}{k_1}) - \theta]} = k_1\, dt \tag{7}$$

This equation is further rearranged for integration:

$$\frac{d\theta}{\theta} + \frac{d\theta}{\frac{k_1 - k_2}{k_1} - \theta} = (k_1 - k_2)\,dt \tag{8}$$

and integration gives:

$$\ln\left(\frac{\frac{k_1 - k_2}{k_1} - \theta}{\theta}\right) = -(k_1 - k_2)t + \ln c \tag{9}$$

where ln c is the constant of integration. Hence,

$$\frac{\frac{k_1 - k_2}{k_1} - \theta}{\theta} = c\,e^{-(k_1 - k_2)t} \tag{10}$$

and

$$\theta = \frac{k_1 - k_2}{k_1}\,\frac{1}{1 + c\,e^{-(k_1 - k_2)t}} \tag{11}$$

It should be noted that the removal rate constant k_2 must be smaller than the growth rate constant k_1 in all cases where the fouling rate is positive. For positive fouling Eq. (6) requires $k_1 > k_2$, given that $\theta \leq 1$, and hence that $\theta(1- \theta) < \theta$. This can further be illustrated by Eq. (11), that is, if and only if $k_1 > k_2$, can θ be positive, and hence fouling is likely. However, the removal process can be significant in some cases, which means that the removal rate constant, k_2 could be close to or even larger than k_1. This will be discussed later.

The initial surface condition determines θ at t = 0. In most cases, θ is finite or very small, but it is not zero at t =0. This requires c to be large assuming the removal rate constant k_2 to be much smaller than the positive growth rate constant k_1. This can be explained by assuming that a few very active spots are formed and occupied by the foulant instantaneously once the heat transfer surface is contacted with the fluid. In the extreme, the initial θ value could either be large (i.e. close to unity) or very small depending on whether the surface is extremely wetting or extremely non-wetting, respectively. In these two extreme cases, the value of c would be very small or very large, respectively. According to Eq. (11), the surface coverage reaches its maximum, $\theta_{max} = (k_1-k_2)/k_1$, when time is infinite.

The integration constant c may be related to the surface characteristics, such as the material, its roughness, charge, wettability, etc, as well its history of use and the properties of the fouling fluid. In general, it needs to be large. Therefore, at the beginning of a fouling process, when t is close to zero, θ is approximately equal to $1/c$, assuming that k_1 is significantly larger than k_2. This gives the physical meaning to the constant c in that $1/c$ is the initial fractional surface coverage.

2.2 Typical θ profiles and length of the induction period

Fig. 1 shows some typical hypothetically calculated profiles of the surface coverage θ against time t. Typically, at the beginning the rate of increase in θ is small. However, this rate increases with time. At a certain point, that is when $\theta = 0.5\ \theta_{max}$, the rate of change of θ with time reaches its maximum, as does the rate of increase in fouling rate with time according to Eq. (1) if the fouling rate R_f' is taken to be constant. In most cases, this is true. That is, fouling is linear especially in the early stages of increasing heat transfer resistance. This means that at $t_{0.5}$, R_f is at a turning point. It is at this point that the fouling is expected to become noticeable, the extent of which depends of course on foulant properties such as its thermal conductivity. Accordingly, it is useful to introduce the term $t_{0.5}$ to define the time when θ reaches its value of $0.5\ \theta_{max}$. Hence $t_{0.5}$ can be used as a measure of the duration of the induction period. Given now that we are interested in $\theta = 0.5\ \theta_{max}$, we have according to Eq. (11):

$$t_{0.5} = \frac{\ln c}{k_1 - k_2} \tag{12}$$

In fact, the surface coverage is very low in the early stages of the induction period as shown in Fig. 1, so that the impact of deposit growing on top of already existing deposit at a possibly different rate would be negligible. In Fig. 1, c is taken arbitrarily to be equal to 10,000 simply as a large enough number, and k_2 is arbitrarily taken to be 0.2. For the solid line in this hypothetical example when k_1 is equal to 5.0 hour^{-1}, $t_{0.5}$ is equal to 1.33 hours. For the dotted line when k_1 is equal to 7.0 hour^{-1}, $t_{0.5}$ is equal to 1.95 hours. Hence, a lower value of k_1 results in a longer induction period.

3. MODEL APPLICATION AND DISCUSSION

3.1 Effect of temperature

It is assumed in the cases of significant fouling that the adhesion/attachment process is much faster than any removal process in the induction (or initiation) period. Hence, the induction (or initial attachment) step is almost irreversible in this period. Consider the following argument. Covering the surface may significantly reduce the system free energy G and, hence, if fouling does occur the irreversibility assumption is understandable. In these cases, the removal effect can be negligible, i.e. k_2 is negligible. k_1 is the lumped growth rate constant which may be assumed to depend on the surface temperature according to the Arrhenius equation:

$$k_1 = A_i \, e^{-E_i / RT} \tag{13}$$

Here, E_i is the activation energy for the induction or surface preconditioning phenomenon and A_i is the pre-exponential factor. Given the relationship between k and T shown in Eq. (13), k_1 would increase with increasing surface temperature, thereby making the induction period shorter. This prediction is in agreement with reported data [4, 10, 13]. Given a negligible value for k_2, substituting k_1 in Eq. (12), using Eq. (13), and then taking logarithms gives the temperature dependency of the induction period:

$$\ln t_{0.5} = \ln(\ln c) - \ln A_i - \frac{-E_i}{RT} \tag{14}$$

The model is now applied to three quite different fouling systems: crude oil, crystallization, and protein fouling. In these case studies it is assumed that k_2 is negligible.

3.1.1 Crude oil fouling

The induction period model was applied to the experimental results obtained in the laboratory at Bath using a batch stirred cell system designed on the basis of Eaton's patent [14]. The design and operation of the apparatus are described elsewhere [15, 16]. The three test probes A, B and C, which were made of mild steel, were polished and their roughnesses measured to be $R_a \approx 10$ μm for probes A and B, but much lower at $R_a \approx 3$ μm for probe C.

All fouling data reported in this work were conducted at constant heat flux and constant interface temperature using test probe A but the effect of using the smoother probe C will be reported later in the paper. It was found that there was always an induction period prior to measurable fouling if the experiment was started with a fresh probe. After the induction period, the fouling resistance was almost always seen to be in a near-linear form with time. In this case, the overall fouling rate can be simply expressed as θ times the constant rate. Hence, the model fit of the fouling resistance was the integration of the overall fouling rate against time. This was carried out numerically.

Fig. 2 shows the model fit to the data of the experiment of a fouling run of Crude B in the stirred cell system. The surface temperature of the heated probe was 376°C and the batch cell was operated with a stirrer speed of 200 rpm (3.33 Hz) giving a surface shear stress predicted by CFD simulation of 0.52 Pa [16]. The data points indicate the experimental fouling data whilst the thin and thick lines represent the θ profile and the model fit, respectively. The model constants k_1 and c were determined by curve fitting the data and were found to be 6.03 hour^{-1} and 8800, respectively. The value of $t_{0.5}$ was found to be equal to 1.51 hours.

Fig. 3 shows the model fitted to the experimental data for the same crude oil but at the higher surface temperatures of 385°C and 411°C. The stirrer speed was unchanged and so the surface shear stress was little changed. A comparison of Figs. 2 and 3 reveals, as expected, that the fouling rate increases with increasing surface temperature. For the data fits in Fig. 3, c values obtained by curve fitting were found to be almost the same as for the data shown in Fig. 2. To keep matters simple therefore, a common value of c = 8800 was chosen for all three temperatures whilst the value of k_1 was allowed to change. For 385°C, k_1 = 6.41 hour^{-1} and $t_{0.5}$ = 1.42 hours. For 411°C, k_1 = 11.9 hour^{-1} and $t_{0.5}$ = 0.76 hours. The error in the R_f measurement could be ± 0.005 m^{2}K/kW, which is mainly caused by the heating power and stirring speed fluctuations, and by random partial shearing off of the deposit.

In summary, $t_{0.5}$ has been calculated to be 1.51, 1.42, and 0.76 hours at 376, 385, and 411°C, respectively. At these time points, inspection of Figs. 2 and 3 confirms that fouling

has become noticeable, thereby demonstrating the value of $t_{0.5}$ as a parameter which provides a practical measure of the length of the induction period.

Plotting $\ln(t_{0.5})$ against $1/T$ using the data of induction period at the three surface temperatures, gives a fair straight line, as seen Fig. 4. This plot indicates that a higher temperature leads to a shorter induction period. The fair linearity of the plot supports the model assumptions. From Fig. 4, the activation energy for the induction period is calculated to be 78.2 kJ/mol. This value is useful for the predicting the effect of surface temperature on the length of induction period.

Fig. 5 shows the model fit to the experimental fouling data using Crude A. Here, the surface temperature was 378°C and the stirrer speed was 100 rpm (1.67 Hz). With the same value of c as for Crude B (8800), the model provides an excellent fit of the fouling data including the induction period with k_1 = 5.68 hour^{-1} and $t_{0.5}$ = 1.6 hours. The value of k_1 is slightly lower than that for the Crude B at a similar surface temperature.

All the fouling data presented in Figs. 2, 3, and 5 were obtained with an initially well-cleaned heated test probe surface. In all these cases, the induction period was clearly observed. In other experimental runs, the probe was not removed from the batch stirred cell for thorough cleaning but was cleaned in-situ. In this case, the authors are doubtful whether the probe surface would have been restored to its perfectly clean condition. In one such case, Fig. 6 shows that an induction period is not observable. The θ profile is shown as the thin line and the model fit to the experimental data is shown as before. The surface temperature was 369.5°C and the stirrer speed was 300 rpm (5 Hz). With a considerable reduction in the value of c down to 1.6, the other model parameters are k_1 = 5.68 hour^{-1} and $t_{0.5}$ = 0.1 hours. The initial surface coverage is calculated to be 0.38.

Fig.6 demonstrates that the model is capable of fitting fouling data that shows no induction period, or a very short induction period. Interestingly, the best fitting was obtained with the same k_1 value as for the fouling run with a well-cleaned probe but with a significantly reduced value of c. This is as expected since in the same experimental system of probe, crude oil and surface temperature, the value of k_1 should remain constant. However,

because the probe surface was not thoroughly cleaned, the initial surface coverage is expected to be much more significant and this is manifested in the much lower value of c.

3.1.2 Crystallization fouling

Fig. 7 shows the fitting of the present model for Förster et al.'s [17] fouling resistance data. The model parameters were c = 14290, k_1 = 0.114 hour^{-1}, and $t_{0.5}$ = 83.9 hours. The fouling rate was set to be linear with stepwise reduction according to the shape of the fouling curve. The model has also been fitted successfully to other published inorganic fouling data. As an example, the model has been fitted to the fouling due to deposit formation in the heat exchangers of an industrial sulphuric acid evaporation plant reported by Müller-Steinhagen and Lancefield [18].

Induction periods in inorganic fouling are, in much the same way as in hydrocarbon fouling, dependent upon many parameters which can be sub-divided into the process conditions and the interface conditions [3].

3.1.3 Protein fouling

Fouling curves as a function of surface temperature for whey protein fouling as obtained by Augustin et al. [4] are shown in Fig. 8. The experimental data shows how the surface temperature affects the length of the induction period. The solid lines show, in addition, how well the new model fits the experimental data. The data were obtained directly from the figure in the original paper but were truncated, showing only the data in the early stages, including the induction period and the linear part of fouling curves. In Fig. 8, ▲ represents data for a surface temperature of 69.8°C for which the model fitting parameters were k_1 = 0.86 hour^{-1}, c = 6466 and $t_{0.5}$ = 10.2 hours. The symbol ■ represents data for a surface temperature 75.7°C, the model parameters being k_1 = 1.18 hour^{-1}, c = 6466, $t_{0.5}$ = 7.4 hours whilst the symbol ♦ represents data for a surface temperature of 81.4°C, the model parameters being k_1 = 1.738 hour^{-1}, c = 6466 and $t_{0.5}$ = 5.05 hours. The results show that, as for crude oil fouling, the length of the induction period reduces as the surface temperature is increased. In turn, it is found that as the surface temperature is increased, the value of k_1 is increased and the value of $t_{0.5}$ is decreased whilst the value of c is held constant at a high value. Since c is related to the initial

surface coverage, it would be expected to be independent of temperature, though further investigation is needed to confirm this.

Fig. 9 shows the dependency of the induction period length on the surface temperature, i.e. a plot of $\ln(t_{0.5})$ against $1/T$. The apparent activation energy is calculated to be 61.2 kJ/mol. Although there are only three data points, the fine linearity of the plot supports the proposed induction period model.

3.2. Effect of velocity

To date, the removal or release terms in fouling models have been difficult to characterize due to the fundamental difficulty in identifying the physical phenomena involved [19]. A number of researchers attribute foulant removal/suppression mechanisms to the effect of surface shear force [20, 21]. Further analysis of the removal term is given by Polley et al. [22] and Yeap et al. [19], suggesting that the removal term is proportional to the 0.8 power of velocity. If this concept is adopted then the removal parameter k_2 in the induction period model may be expressed as follows:

$$k_2 = \gamma u^{0.8} \tag{15}$$

Here γ is a constant and u is velocity. Given this relationship, the surface coverage would remain at a very low level according to Eq. (11) and the induction period would be extremely long or even infinite if the velocity were to be sufficiently high. Experimental results of crude oil fouling using the stirred cell system [15] at high stirrer speeds showed no fouling even after running for a considerably long period (accordingly, detailed results cannot therefore be reported). This was likely due to a long induction period under high stirrer speed. Published experimental results relating to the effect of velocity on induction period time, even though they are relatively limited to date, are now used to test the model.

Mwaba et al [23] reported the calcium sulphate crystallization fouling resistance for different velocities, showing a significant extension of the induction period at higher velocity. Applying the proposed model to these data from start up to the end of the linear part of fouling, as shown in their Figure 14, reveals that reasonable fits for the fouling curves can be

obtained, as shown in Fig. 10. The velocity data, induction period time, and model parameters obtained by regression are listed in Table 2. Notably, the induction times calculated using Eq. (12) are in fair agreement with those observed in the experiments.

Geddert et al. [3] were interested in extending the induction period of crystallization fouling by the application of various surface coatings onto stainless steel. Coatings extended the induction period in calcium sulphate scaling for every flow velocity studied. Indeed, the induction period could be extended to about 23 hours using SICON coating for a low fluid velocity of Reynolds number of 1030, and to about 65 hours using the same coating for a higher velocity of Reynolds number of 3010. Fouling resistance data for stainless steel and SICON coating, up to the end of linear part shown in Figs. 17 and 18, respectively, of Geddert et al. [3] were selected to evaluate the new induction period model. These data are selected simply because the two data sets clearly demonstrate the effects of both coating and velocity on fouling induction time. In this case, Reynolds numbers are used instead of velocity. The model fits for these data are shown in Fig. 11, demonstrating that the model is capable of closely following the trend of the fouling resistance against time. The model parameters are listed in Table 3. The SICON coating significantly altered the values of both c and k_1, but did not significantly alter k_2.

Further studies of the effect of velocity may reveal the velocity dependency of k_1, if the growth of surface coverage is mass transport controlled. In contrast to Geddert et al.'s study, the induction period has been seen to be shortened by an increase in velocity [24]. If it is the case that increased velocity can either increase or reduce the duration of the induction period then the deposit growth term in models such as that proposed by Yeap et al. [19] might be useful in defining the parameter k_1. This is because this expression shows a maximum in the k_1 versus velocity relationship:

$$k_1 = \frac{AC_f\, uT^{2/3}\rho^{2/3}\mu^{-4/3}}{1 + Bu^3 {C_f}^2 \rho^{-1/3}\mu^{-1/3}T^{2/3}\exp(E/RT)} \tag{16}$$

However, whilst this model can account for the maximum in the fouling rate – velocity relationship, the model contains so many parameters that large amounts of experimental

fouling resistance data would be required to determine them all by regression. Indeed, insufficient data are available at the moment to validate whether Yeap's model could be used in a general manner for the interpretation of induction period data. Nonetheless, this could become the subject of further studies. It should be noted that the parameters involved in k_1 and k_2 for induction period could well differ from those in the fouling rate model used to account for noticeable fouling since the reaction, if indeed there is any in the induction period, would be between the foulant and the metal surface of the heat exchanger rather than between the foulant and the deposit that adheres to the heat transfer surface.

3.3 Effect of surface properties and other factors

Whilst surface properties can have a significant influence on the induction period [3, 25], it is difficult to incorporate them within fouling models. Firstly, the mechanisms by which some surface properties, such as surface energy, affecting fouling is unclear, and secondly some surface properties, such as surface roughness for instance, change dynamically while the surface is gradually being covered by foulants. Geddert et al. [3] investigated the induction time of crystallisation fouling on different surfaces and concluded that the comparison of total surface energy data with induction time yields no correlation between surface energy and fouling behaviour. They attributed the extension of an induction time using a surface coating to its lowered adhesive level, a parameter which is not easily capable of being measured quantitatively. Qualitatively however, a low adhesive surface will give a larger value of c, and a smaller value of k_1, which can result in a longer induction time, as described in section 3.2.

Heat transfer can be enhanced by an increase in surface roughness [26] and hence can lead to apparently negative fouling during the induction period. In this paper, negative fouling during induction periods is not considered in the model development, due to the difficulty in following the dynamic change of the surface roughness during the induction period. However, a higher initial surface roughness could well favour fouling growth, and hence reduce the induction time. Experiments on crude oil using two test probes that have different initial surface roughnesses indeed show that the induction time was significantly longer using the

lower roughness probe C than the higher roughness probe A [15]. The higher surface roughness is believed to give a larger *c* value. However, no quantitative correlation has been established [15].

Other factors including fluid composition and bulk temperature may have an influence on the induction time. In fact, any factor that favours fouling could reduce the length of the induction period. For instance, crude oils with higher asphaltene contents could foul faster than those with low asphaltene contents [15]. The effect of composition could possibly be incorporated in the parameter k_1. The same argument may apply to bulk temperature.

3.4 Induction period and fouling thresholds

Here, only crude oil will be considered. Fouling threshold phenomena [12, 21] could be interpreted using Eqs. (11) and (12). That is, if k_2 is close to k_1, surface coverage may remain sufficiently low, or the induction period may be infinite, and hence a boundary could be drawn between the fouling zone in which $k_1 > k_2$, and the non-fouling zone in which $k_1 < k_2$. Assuming that the fouling threshold concept is a valid one for crude oil, then a heat exchanger, such as one in the crude preheat train in an oil refinery [15], could ideally be operated in the non-fouling zone, or at least fairly close to the threshold, which means that k_2 would be of the same order as k_1. If this were to be the case, and the running time were to be sufficiently long, then the surface coverage would be close to its maximum, i.e. $(k_1-k_2)/k_1$, and the fouling rate would be according to Eq. (1):

$$\frac{dR_f}{dt} = \frac{k_1 - k_2}{k_1} R_f' \tag{16}$$

If k_2 was of the same order as k_1, i.e. $(k_1-k_2)/k_1 < 1$ or $<< 1$, then the actual fouling rate would be significantly lower than R_f' which is predicted by the fouling rate models. This means that fouling behaviour at or near a threshold could be significantly different from that far above the threshold where the maximum coverage, $(k_1-k_2)/k_1$ would be close to unity. Given that k_2 is related to velocity or shear stress, as is the fouling rate, R_f', an increase in

velocity should have a much stronger effect on the fouling rate if the operating conditions are fairly close to the threshold.

Andersson et al. [27] reported fouling resistance results in the pre-heat train of an oil refinery. Predicted fouling resistances were much higher than the actual values when the heat exchanger was operated under a higher flow velocity, as seen in Fig. 12. Although no fouling rates are given, the gradient of the curve of predicted resistance with time is greater than that for the actual resistance curve. A similar case can be seen in Fig. 5 of Polley and Gonzales-Garcia [28], suggesting again that the predicted fouling rate was greater than the actual. Polley et al. [29] compared the model predicted fouling rates with the measured rates in three field operation cases. In one case, the predicted rate was 50% higher than the measured value, while in another case, the predicted rate was 20% above the measured value. In the final case, the initial rates coincided, but the predicted rate fell away more rapidly than the measured performance, and after 6000 hours, the predicted level was about 60% of the measured level. Asomaning et al. [30] attempted to correlate field and laboratory data for crude oil fouling, and pointed out that the model developed using laboratory data predicts data from the field unit with a limited degree of success. Eq. (16) could offer a possible or partial explanation for differences between the predicted and actual measured fouling rates. However, further collection and analysis of fouling rate data, especially from fields, are needed in order to draw a firm conclusion.

4. CONCLUSIONS

The new model proposed in this paper makes it possible to describe the fouling process from the start of the induction period up to the steady fouling rate stage using a single and simple mathematical expression. The model has been tested on experimental data for crude oil fouling, calcium sulphate fouling and whey protein fouling. The proposed term $t_{0.5}$ which is the time to reach 50% of the maximum surface coverage, θ_{max}, provides a practical measure of the length of the induction period. The model quantitatively describes the influence of the surface temperature on the length of the induction period for the crude oil and whey protein fouling systems. The model also describes in a semi-quantitative manner the influence of

velocity on the induction time. Much more research needs to be carried out on the effect of velocity because its effect is much more complex than that of surface temperature. The influences of other important factors, such as surface adhesive level and surface roughness, are also difficult to incorporate quantitatively in the model. Further research therefore needs to be focussed on incorporating in the model parameters k_1 and k_2 as many as possible of the physical and chemical properties that influence deposition, attachment and removal in specific applications.

ACKNOWLEDGEMENTS

The authors are grateful to the UK's Engineering and Physical Sciences Research Council (EPSRC) for the award of a research grant (EP/D506131/1) to study the role of asphaltenes in crude oil fouling. The authors are grateful also to their EPSRC project partners at Imperial College London and the University of Cambridge, as well as to ExxonMobil and Petronas who supplied samples of crude oils.

REFERENCES

[1] Belmar-Beiny M. T. Gotham S.M., Peterson W. R.., Fryer P. J., and Pritchard A. M., The effect of Reynolds number and fluid temperature in whey protein fouling *J. Food Eng*. 19 (1993), 119-139.

[2] Belmar-Beiny M. T. and Fryer P. J., Preliminary stages of fouling from whey protein solutions, *J. Dairy Res*. 60 (1993), 467 – 483.

[3] Geddert T., Bialuch I., Augustin W., and Scholl S., Extending the induction period of crystallization fouling through surface coating, *Heat Transfer Engineering*, 30: 10-11, (2009) 868-875.

[4] Augustin, W., Geddert, T., and Scoll, S., Surface treatment for the mitigation of whey protein fouling. *Proceedings of the 7th International conference of Heat Exchanger Fouling and Cleaning,* eds. H. Müller-Steinhagen, M. Reza Malayeri and A. P. Watkinson, Engineering Conferences International, New York, 2007, pp. 206-214.

[5] Wilson, D. I., Polley, G. T., and Pugh, S. J., Ten years of Ebert, Panchal and the 'Threshold Fouling Concept'. *Proc. 6th International Conference on Heat Exchanger Fouiling*

and Cleaning: Challenge and Opportunities. Eds. H. Müller -Steinhagen, M. Reza Malayeri and A. P. Watkinson, Engineering Conferences International, Kloster Irsee, Germany, 2005, pp. 25-36.

[6] Vatistas, N., 1987, *Fouling Science and Technology*. Eds. L. F. Melo, T. R. Bott, and C. A. Bernardo, Kluwer Academic Publishers, Dordrecht, 1987, pp.165-172.

[7] Malayeri, M. R. and Müller-Steinhagen, H., Initiation of $CASO_4$ scale formation on heat transfer surface under pool boiling conditions. *Heat Transfer Engineering*, 28 (2007), 240-247.

[8] Radhakrishnan, V. R., Ramasamy, M., Zabiri, H., Thanh, V. Do, Tahir, N. M., Mukhtar, H., Hamdi, M. R., and Ramli, N., Heat exchanger fouling model and preventive maintenance scheduling tool. *Applied Thermal Engineering*, 27 (2007), 2791-2802.

[9] Fahiminia F., Watkinson A. P. and Epstein N., Calcium sulfate scaling delay times under sensible heating conditions, *Proceedings of the 7th International conference of Heat Exchanger Fouling and Cleaning*, , eds. H. Müller-Steinhagen, M. Reza Malayeri and A. P. Watkinson, Engineering Conferences International, Kloster Irsee, 2005, pp.310-315.

[10] Crittenden, B. D, Kolaczkowski, S. T., and Hout, S. A., Model experiments of chemical reaction fouling. *Chem. Eng. Res. Des*., 65 (1987), 165-170.

[11] Epstein N., Initial chemical reaction fouling rate for flow through a heated tube, and its verification. *Proc. 10th Int. Heat. Transfer. Conference.*, Brighton, IChemE, 1994, Vol. 4, pp.225-229.

[12] Ebert, W. and Panchal, C. B., Analysis of Exxon crude-oil slip stream coking data. *Fouling Mitigation of Industrial Heat Exchange Equipment*, eds. C. B. Panchal,, R. T. Bott, E. F. C. Somerscales, and S. Toyama, Begell House, New York, 1997, pp.451-460.

[13] Saleh Z S., Sheikholeslami, R. and Watkinson, A. P., Fouling characteristics of a light Australia crude oil. *Heat Transfer Engineering*, 26 (2005), 15-22.

[14] Eaton P, Fouling test apparatus, US patent 4383438, 1983.

[15] Young A., Venditti S., Berrueco C., Yang M., Waters, A., Davies H., Hill, S., Millan M. and Crittenden B. D., Characterisation of crude oils and their fouling deposits, *Heat Transfer Engineering* 32 (2011), 216-227.

[16] Yang M., Young, A., and Crittenden B. D., Use of CFD to correlate crude oil fouling against surface temperature and surface shear stress in a stirred fouling apparatus. *Proc. Eurotherm Conference of Heat Exchanger Fouling and Cleaning*, Schladming, Austria, 2009, pp.272-280.

[17] Förster, M., Augustin, W., Bohnet, 1999, M., Influence of the Adhesion Force crystal/Heat Exchanger Surface on Fouling Mitigation, *Chem. Engng. Process.*, 38, (1999), 449-461.

[18] Müller-Steinhagen, H. and Lancefield, D., Deposit formation in the evaporator of a sulfuric acid recovery plant for TiO_2 pigment production. *Heat Transfer Engineering*, 28 (2007), 210-216.

[19] Yeap, B. L., Wilson, D. I., Polley, G. T., and Pugh, S. J., Mitigation of crude oil refinery heat exchanger fouling through retrofits based on thermo-hydraulic fouling models. *TransIChemE Part A*, 82 (2004), 53-71.

[20] Polley, G.T., Wilson, D.I., Yeap, B.L. and Pugh, S.J., Use of crude oil threshold data in heat exchanger design, *Appl Therm Eng*, 22, (2002), 763–776.

[21] Panchal, C.B., Kuru, W.C., Liao, C.F., Ebert, W.A. and Palen, J.W., Threshold conditions for crude oil fouling, in Understanding Heat Exchanger Fouling and its Mitigation, Bott, T.R., Melo, L.F., Panchal, C.B. and Somerscales, E.F.C. (eds), Begell House, New York, USA, 1999, pp 273–279.

[22] Polley, G.T., Wilson, D.I., Yeap, B.L. and Pugh, S.J., Evaluation of laboratory crude oil fouling data for application to refinery pre-heat trains, *Appl Therm Eng*, 22, (2002), 777–788.

[23] Mwaba, M. G. , Rindt, C. C. M. , Van Steenhoven, A. A. and Vorstman, M. A. G. Experimental Investigation of CaSO4 Crystallization on a Flat Plate, *Heat Transfer Engineering*, 27: 3, (2006), 42 – 54.

[24] Yang, Q. F., Liu, Y. Q., Gu, A. Z., Ding, J. And Shen, Z. Q., Investigation of induction period and morphology of $CaCO_3$ fouling on heated surfaces, *Chemical Engineering Science*, 57, (2002), 921-931.

[25] Geddert T., Augustin W., and Scholl S., Influence of surface defects and aging of coating surfaces on fouling behaviour, *Heat transfer Engineering*, 32: 3-4, (2011), 300-306.

[26] Albert, F, Augustin, W., and Scholl, S., Enhancement of heat transfer in crystallization fouling due to surface roughness, *Proc. Eurotherm Conference of Heat Exchanger Fouling and Cleaning*, Schladming , Austria, 2009, pp.303-310.

[27] Andersson, E., Quah, J., and Polley, G.T., (2009), Experience in application of Compabloc™ heat exchangers in refinery pre-heat trains, *Proc. Eurotherm Conference of Heat Exchanger Fouling and Cleaning*, Schladming , Austria, 2009, pp. 39-43.

[28] Polley, G. T. and Gonzales-Garcia, Procedure for applying fouling models to predict overall fouling rates in industrial heat exchagers, *Proc. Eurotherm Conference of Heat Exchanger Fouling and Cleaning*, Schladming , Austria, 2009, pp. 362-366.

[29] Polley, G. T., Wilson, D. I., Pugh, S. J. and Petitjean, E., Extraction of Crude Oil Fouling Model Parameters from Plant Exchanger Monitoring, *Heat Transfer Engineering*, 28, (2007) 185-192.

[30] Asomaning, S., Panchal, C. B., and Liao, C. E., Correlation of field and laboratory data for crude oil fouling, *Heat Transfer Engineering*, 27, (2000), 17-23.

Table 1 Functions of R_f' used for the fouling rates in related figures

R_f' [$m^2K/(kJ)$]	Applications and conditions	Figure number	Reference
3.06E-6	Crude B, 376°C	Fig. 2	Young et al. [15]
5.28E-6	Crude B, 385°C	Fig. 3	Young et al. [15]
6.67E-6	Crude B, 411°C	Fig. 3	Young et al. [15]
4.33E-6	Crude A 378°C	Fig. 5	Young et al. [15]
7.78E-7	Crude A, 369.5°C	Fig. 6	Young et al. [15]
(5.6E-9) – (1.9E-11)*t	Crystallization	Fig. 7	Geddert et al. [3]
2.03E-8	Whey	Fig. 8	Augustin et al. [4]
2.06E-8	Whey	Fig. 8	Augustin et al. [4]
2.47E-8	Whey	Fig. 8	Augustin et al. [4]

t: time (hour)

Table 2 Model parameter for fitting of MWaba et al. data [23]

Velocity (m/s)	k_1 (1/min)	k_2 (1/min)	γ ($m^{-0.8}s^{-0.2}/60$)	c	$t_{0.5}$ (min) observed	$t_{0.5}$ (min) model
0.3	0.00618	0.00170	0.00456	2480	1210	1760
0.6	0.00618	0.00303	0.00456	2480	2490	2480
1.0	0.00618	0.00456	0.00456	2480	4640	4840

Table 3 Model parameters for fitting of Geddert et al.data [3]

Coating	*Re*	k_1 (1/hour)	k_2 (1/hour)	γ	c	$t_{0.5}$ (hour) observed	$t_{0..5}$ (hour) model
No coating	1030	2.57	0.33	0.0013	1400	3	3.2
No coating	3010	2.57	0.79	0.0013	1400	4	4.1
SICON	1030	0.66	0.196	7.61E-4	251000	23	26
SICON	3010	0.66	0.462	7.61E-4	251000	65	63

List of Figure Captions

Fig. 1 Typical θ profiles

c = 6400

Fig. 2 Model application to Crude B with a heated probe surface temperature of 376°C, bulk temperature: 250°C, pressure: 30 bar, and average heat flux: 106 kW/m^2

Fig. 3 Model application to Crude B crude

Bulk temperature: 250°C, pressure: 30 bar

■: surface temperature 385°C, average heat flux 110 kW/m^2; ▲: Surface temperature 411°C, average heat flux: 116 kW/m^2; Lines: model fits.

Fig. 4 Temperature dependence of the model constant k_1

Fig. 5 Model application to Crude A

Surface temperature 378°C, bulk temperature: 25°C, average heat flux 92 kW/m^2

Thin line: θ profile; Thick line: model fits

Fig. 6 Model application to Crude A with an imperfectly cleaned probe surface

Surface temperature 355°C, bulk temperature: 250°C, pressure: 30 bar, average heat flux 88 kW/m^2

Thin line: θ profile; Thick line: model fits

Fig. 7 Model application to the fouling data reported by Förster et al. [17]

Thin line: θ profile; Thick line: model fit

Fig. 8 Model application to whey protein fouling data reported by Augustin et. al. [4]

▲: experimental data at surface temperature of 69.8°C, for which the model fitting (line) parameters were k_1 = 0.86 hour^{-1}, c = 6466 and $t_{0.5}$ = 10.2 hours.

■: experimental data at a surface temperature 75.7°C, the model parameters being k_1 = 1.18 hour^{-1}, c = 6466, $t_{0.5}$ = 7.4 hours.

♦: experimental data at a surface temperature of 81.4°C, the model parameters being k_1 = 1.738 hour^{-1}, c = 6466 and $t_{0.5}$ = 5.05 hours.

Fig. 9 Temperature dependence of the model constant *k* for the whey protein fouling reported by Augustin et. al. [4]

Fig. 10 Effect of velocity - Model fittings for Mwaba et al. data [23]

From left to right: 0.3 m/s, 0.6 m/s, 1.0 m/s

Symbols: Mwaba experimental data; Lines: model fittings

Fig. 11 Model fittings for Geddert et al. data

From left to right: Stainless steel Re 1030, Re 3010, SICON coating Re 1030, Re3010

Symbols: Geddert et al. data; Lines: model fittings

Fig. 12 Fouling resistance against time (After Figure 3 in Andersson et al. [27])

Rd: fouling resistance (m^2K/W)

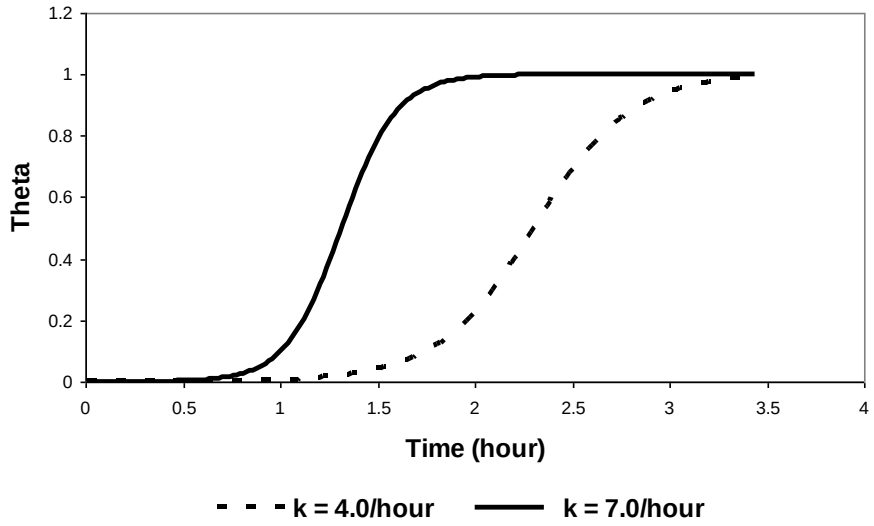

Fig. 1 Typical θ profiles

c = 6400

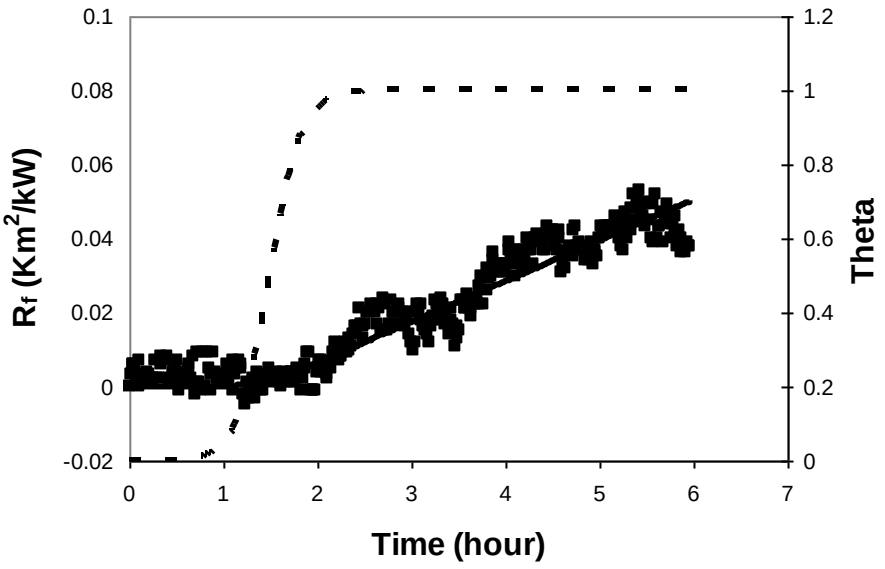

Fig 2. Model application to Crude B with a heated probe surface temperature of 376°C, average heat flux: 106 kW/m^2 [15].

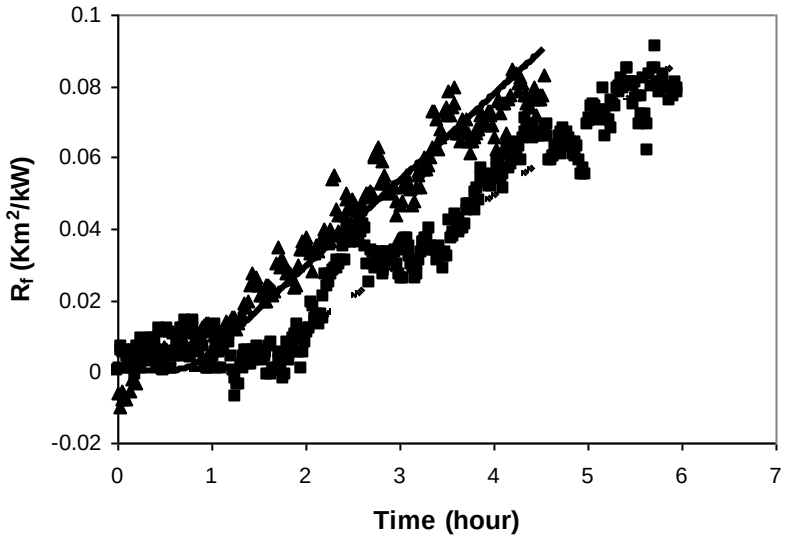

Fig 3. Model application to Crude B crude [15]

■: surface temperature 385°C, average heat flux 110 kW/m^2; ▲: Surface temperature 411°C, average heat flux: 116 kW/m^2; Lines: model fits.

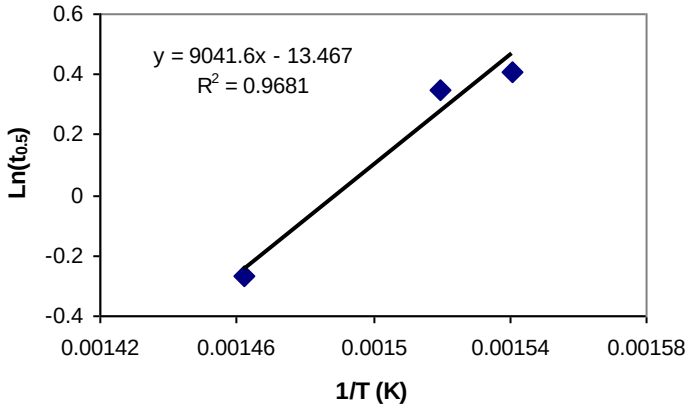

Fig. 4 Temperature dependence of the induction time for crude oil fouling [15].

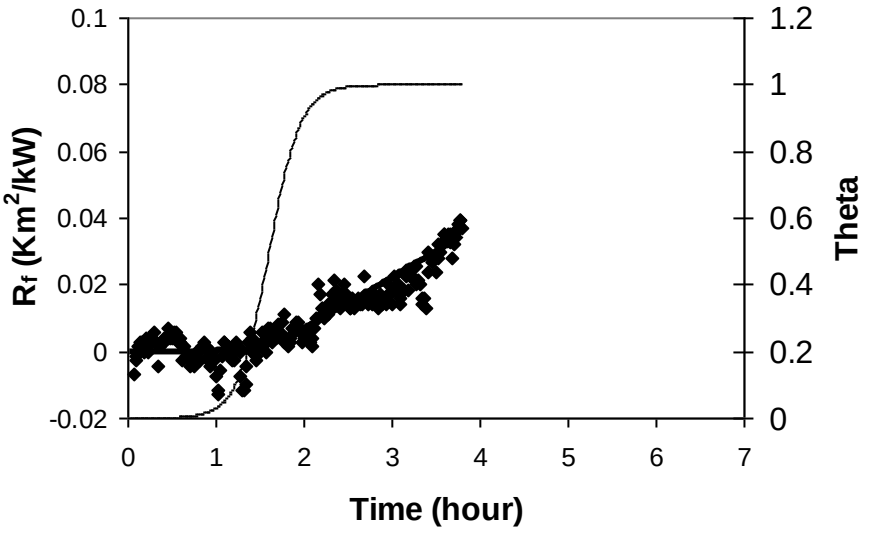

Fig. 5 Model application to Crude A [15].

Surface temperature 378°C, average heat flux 92 kW/m^2

Thin line: θ profile; Thick line: model fits

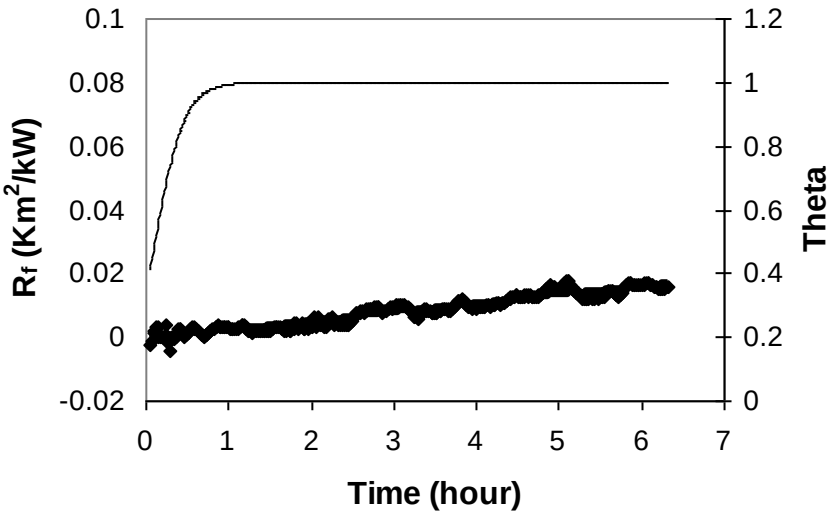

Fig. 6 Model application to Crude A with an imperfectly cleaned probe surface [15].

Surface temperature 355°C; Average heat flux 88 kW/m^2

Thin line: θ profile; Thick line: model fits

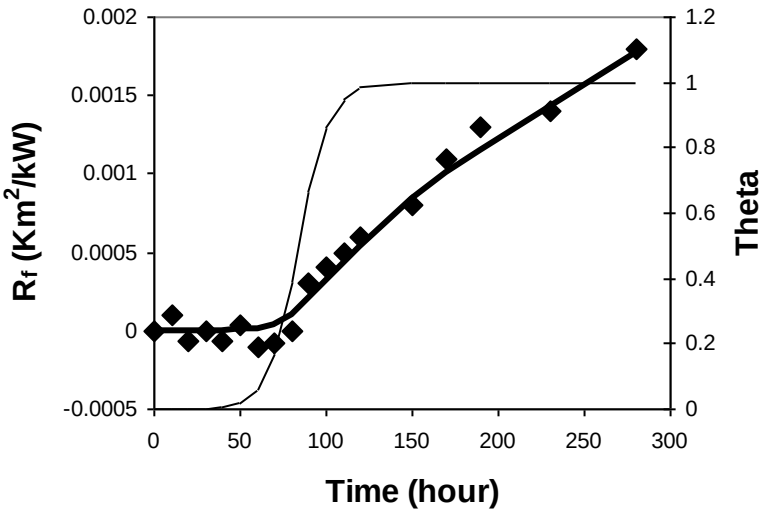

Fig. 7 Model application to the fouling data reported by Förster et al. [17].

Thin line: θ profile; Thick line: model fit

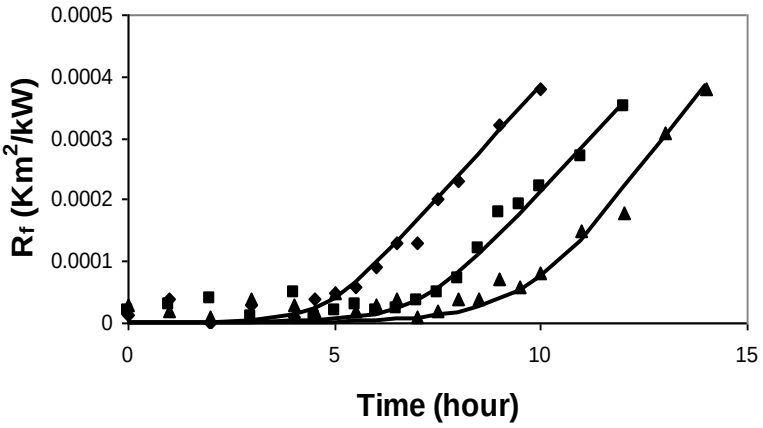

Fig. 8 Model application to whey protein fouling data reported by Augustin et. al. [4].

▲: experimental data at surface temperature of 69.8°C, for which the model fitting (line) parameters were k_1 = 0.86 hour^{-1}, c = 6466 and $t_{0.5}$ = 10.2 hours.

■: experimental data at a surface temperature 75.7°C, the model parameters being k_1 = 1.18 hour^{-1}, c = 6466, $t_{0.5}$ = 7.4 hours.

♦: experimental data at a surface temperature of 81.4°C, the model parameters being k_1 = 1.738 hour^{-1}, c = 6466 and $t_{0.5}$ = 5.05 hours.

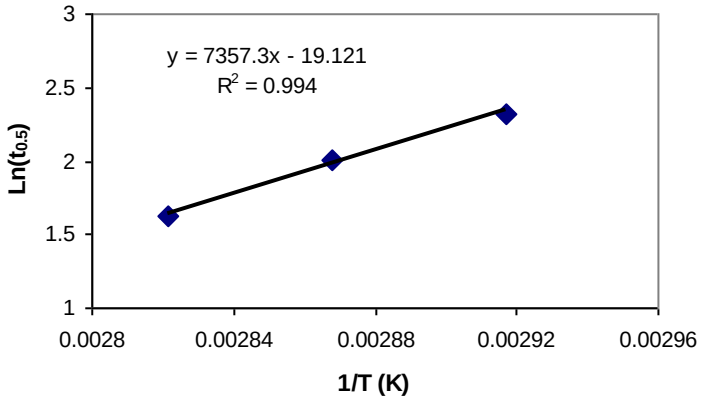

Fig. 9 Temperature dependence of the induction time for the whey protein fouling reported by Augustin et al. [4].

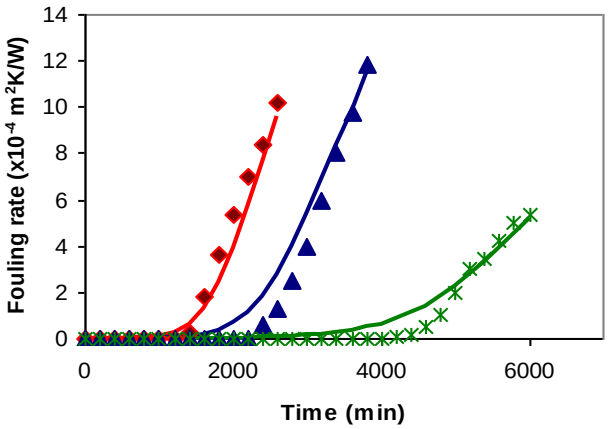

Fig. 10 Effect of velocity - Model fittings for Mwaba et al. data [23].

From left to right: 0.3 m/s, 0.6 m/s, 1.0 m/s

Symbols: Mwaba experimental data; Lines: model fittings

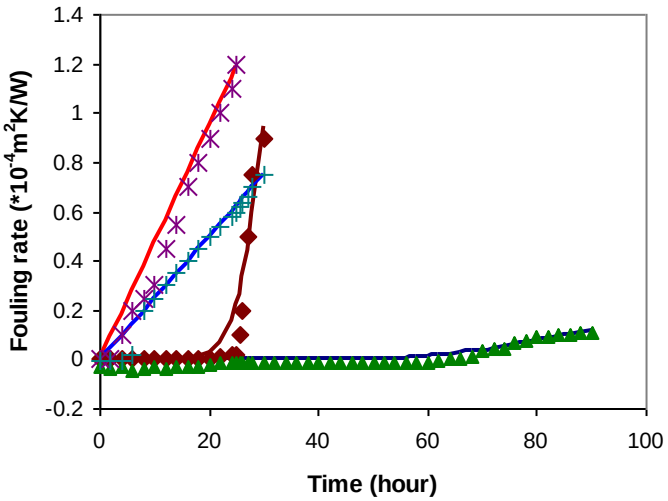

Fig. 11 Model fittings for Geddert et al. data [3].

From left to right: Stainless steel Re 1030, Re 3010, SICON coating Re 1030, Re3010

Symbols: Geddert et al. data; Lines: model fittings

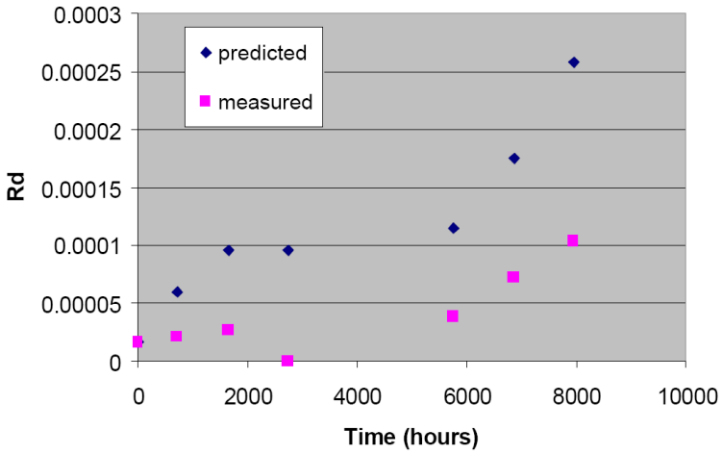

Fig. 12 Fouling resistance against time (After Figure 3 in Andersson et al. [27])

Rd: fouling resistance (m^2K/W)